Nanoscale

Accepted Manuscript

This article can be cited before page numbers have been issued, to do this please use: J. van den Boom, A. Hensel, F. Trusch, A. Matena, S. Siemer, D. Guel, D. Docter, A. Höing, P. Bayer, R. H. Stauber and S. Knauer, *Nanoscale*, 2020, DOI: 10.1039/D0NR01631D.

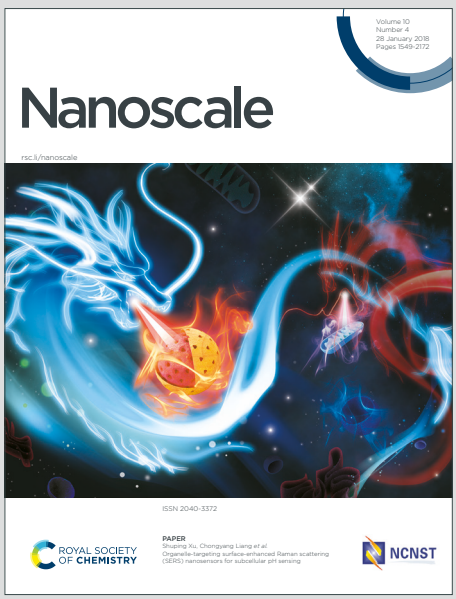

ROYAL SOCIETY OF CHEMISTRY

rsc.li/nanoscale

Nanoscale

View Article Online
DOI: 10.1039/D0NR01631D

ARTICLE

The Other Side of the Corona: Nanoparticles Inhibit the Protease Taspase1 in a Size-Dependent Manner

Received 00th January 20xx,
Accepted 00th January 20xx

DOI: 10.1039/x0xx00000x

Johannes van den Boom,*[a] Astrid Hensel,[b] Franziska Trusch,[a] Anja Matena,[a] Svenja Siemer,[c] Désirée Guel,[c] Dominic Docter,[c] Alexander Höing,[b] Peter Bayer,[a] Roland H. Stauber[c] and Shirley K. Knauer[b]*

When nanoparticles enter a physiological environment, they rapidly adsorb biomolecules, in particular cellular proteins. This biological coating, the so-called nanoparticle protein corona, undoubtedly affects the biological identity and potential cytotoxicity of the nanomaterial. To elucidate a possible impact on the adsorbed biomolecules, we focused on an important group of players in cellular homeostasis, namely proteolytic enzymes. We could demonstrate that amorphous silica nanoparticles are not only able to bind to the oncologically relevant threonine protease Taspase1 as revealed by microscale thermophoresis and fluorescence anisotropy measurements, but moreover inhibit its proteolytic activity in a non-competitive manner. As revealed by temperature-dependent unfolding and CD spectroscopy, binding did not alter the stability of Taspase1 or its secondary structure. Noteworthy, inhibition of protein function seems not a general feature of nanoparticles, as several control enzymes were not affected in their proteolytic activity. Our data suggests that nanoparticles bind Taspase1 as an $\alpha\beta$-dimer in a single layer without conformational change, resulting in noncompetitive inhibition that is either allostery-like or occludes the active site. Nanoparticle-based inhibition of Taspase1 could be also achieved in cell lysates and in live cells as shown by the use of a protease-specific cellular cleavage biosensor. Collectively, we could demonstrate that nanoparticles could not only bind but also selectively inhibit cellular enzymes, which might explain observed cytotoxicity but might serve as a starting point for the development of nanoparticle-based inhibitors as therapeutics.

Introduction

The use of nanomaterials in biomedical and biotechnological applications is growing, and there is also an increasing likelihood that such materials will be released into the environment as consumer products.[1] Due to their high free surface energy, nanomaterials adsorb biomolecules upon contact with biological fluids.[2] In particular, proteins bind the surface of nanoparticles forming a biological coating around the particle known as the protein corona. This corona affects the biological identity of the nanomaterial and may thus affect biomedical applications or modulate nanotoxicological effects, including cytotoxicity. The physico-chemical properties of nanoparticles, and their exposure time to biological environments are discussed to influence the protein corona, affecting the biodistribution of the particles and their therapeutic and pathophysiological effects.

On the other hand, it is certainly not far-fetched to assume that the adsorption might also influence the biological properties and cellular function of the bound biomolecules. One fundamental task of proteins is to act as enzymes that catalyze the rate of virtually all cellular chemical reactions that otherwise would be too slow to be compatible with life.[3] One pivotal subgroup of the large family of enzymes is representing the proteases (also called peptidases or proteinases), which cleave proteins by hydrolyzing peptide bonds (ESI Fig. S1a).[4] Although proteases were initially described as nonspecific enzymes, it is now accepted that this protein family contains key players for the regulation of specific degradation and cleavage processes in all organisms. Undoubtedly, proteolysis is a critical requirement for life, and approximately 600 proteases are present in the human genome classified into five classes according to their active site (serine, cysteine, threonine, aspartate, and metalloproteases; ESI Fig. S1b).[5] Proteolytic activity is crucial for the delicate regulation and timely orchestration of multiple cellular processes. As protease signaling relies on the cleavage of peptide bonds, it can in general be considered as irreversible and thus has to underlie stringent control mechanisms. Consequently, protease deregulation often leads to (patho-) physiological states, marking proteases as important drug targets in the pharmaceutical industry.[6]

[a] Structural and Medicinal Biochemistry, Department of Biology, University Duisburg-Essen and Zentrum für Molekulare Biotechnologie (ZMB), Universitätsstrasse 5, Essen, 45141 Germany.
[b] Molecular Biology II, Department of Biology, University Duisburg-Essen and Zentrum für Molekulare Biotechnologie (ZMB) and Center for Nanointegration Duisburg-Essen (CENIDE), Universitätsstrasse 5, Essen, 45141 Germany
[c] Molecular and Cellular Oncology, University Medical Center Mainz, Langenbeckstrasse 1, Mainz, 55101 Germany.
* Corresponding authors: shirley.knauer@uni-due.de, johannes.van-den-boom@uni-due.de
† Electronic Supplementary Information (ESI) available. See DOI: 10.1039/x0xx00000x

DOI: 10.1039/D0NR01671D

In this respect, Taspase1 (Threonine Aspartase-1), a protease of 420 amino acids (aa) is responsible for activation and stabilization of Mixed-lineage leukemia protein MLL and its oncogenic fusion proteins.[7] Proteolytic processing of the AF4•MLL fusion protein by Taspase1 for example results in a high molecular-weight protein complex resistant to proteasomal degradation, driving oncogenic events.[8] Like the proteasome, Taspase1 belongs to the rather small class of threonine proteases.[9] It is not only an N-terminal threonine endopeptidase with the active site residue located at the β-subunit, but furthermore a member of the type 2 asparaginase family of enzymes (ESI Fig. S1c).[7, 10] All members of this family share the ability to be autocatalytically processed in *cis* (ESI Fig. S1d), albeit Taspase1 is the only family member that functions as a protease cleaving other substrates by recognizing a conserved peptide motif ($Q_3[F,I,L,V]_2D_1\downarrow G_{1'}x_{2'}D_{3'}D_{4'}$) with an aspartate at the P1 position.[11, 12] Mutation of the catalytic nucleophile, Thr234, results in loss of *cis*-activity and also completely abolishes Taspase1's proteolytic function in *trans*.[10, 13] Based on the crystal structures of other type 2 asparaginases as well as on the structure obtained from bacterially expressed Taspase1 (ESI Fig. S1c), it was concluded that the enzyme consists of a four-layered αββα-structure, with a central, mostly antiparallel β-sandwich surrounded by α-helices on both faces. Hence, the proenzyme as well as activated Taspase1 is considered to assemble into an αββα-heterodimer.[13] However, studies clearly showing that Taspase1 and other type 2 asparaginases indeed exist as heterodimers in their natural environment and that multimerization is essential for their biological activities are still missing. The prediction of Taspase1's degradome [12, 14] together with recent experimental evidence further implies that the protease plays not only a crucial role in leukemia, but also in solid tumors.[8, 15, 16] Besides MLL-fusions also other nuclear and cytoplasmic regulatory proteins, such as the precursor of the Transcription Factor IIA (TFIIA)[17] or the upstream stimulating factor 2 (USF2) are *bona fide* Taspase1 targets.[12, 17] Unfortunately, Taspase1's catalytic activity is not affected by common protease inhibitors.[7] Currently, neither genetic nor specific and highly effective chemical inhibitors for this enzyme are available. This not only hampers the further dissection of Taspase1's (patho)biological functions in vivo, but also precludes the assessment of its clinical and therapeutic relevance in vitro and in cell culture.[18, 19] Thus, exploiting novel strategies to inhibit Taspase1 is indeed of utmost importance.

As stated above, it is on the other hand of great importance to evaluate the molecular mechanisms underlying the observed cytotoxicity of nanomaterials. These mechanisms are certainly as intricate and diverse as the nature of the material, with varying sizes and shapes adding even more complexity.[2] Although the biological basis of certain nanomaterials' toxicity is far from being understood, certainly the effectiveness of cell surface binding and eventually cellular uptake contribute significantly. Inside the cell, the capacity of the nanomaterial to interact with physiological proteins and thus the ability to modulate their behavior will be pivotal. This mirrors the corona formation described in biological fluids, thus guided by the same principles. Protein adsorption occurs spontaneously if it is thermodynamically favored.[20] This may lead to conformational changes, especially when hydrophobic or charged protein domains interact with nanomaterial surfaces.[21] Although undoubtedly depending on the characteristics of both the nanomaterial and the protein, it can be assumed that stable proteins are less affected than proteins with highly flexible domains, like loop structures or protruding helices. The latter will more likely lead to the loss of protein activity or at least alter the way in which the protein is presented to its environment - either by exposing normally inaccessible domains or by rearranging critical functional domains. Indeed, nanoparticles are capable of inactivating or modulating proteins such as proteolytic enzymes, the proteasome, cytochrome c, fibrinogen and LDH.[22-29] Only in some cases protein structure was significantly affected, and also the charge as an important determinant could not fully explain the underlying inhibitory mechanism. Collectively, these data indicate that binding specificity of nanomaterials for a distinct (class of) protein(s), and also other biomolecules may exist. Notably, binding constants determined for the adsorption of proteins to nanoparticles were reported to be in the micro- to nanomolar range, comparable to the highly selective and biologically relevant antibody-antigen interactions.[30]

Indeed, here we show that amorphous silica nanoparticles are not only able to bind to an oncologically relevant protease, but moreover selectively inhibit its proteolytic activity in a non-competitive manner. We could also shed light on the underlying molecular mechanism as nanoparticles did not alter protein stability or secondary structure but seem to bind the protease dimer in a single layer occluding the positively charged active site. Moreover, the fact that protease inhibition could be also achieved in cell lysates and in live cells might at least partially explain observed nanoparticle cytotoxicity but on the other hand also serve as a starting point for the development of nanoparticle-based inhibitors as therapeutics.

Results

Nanoparticles bind and inhibit Taspase1 in vitro.

To thoroughly characterize the effects of nanoparticle binding to Taspase1, we first optimized recombinant protein expression and purification for not only wildtype Taspase1, but also an active, already cleaved variant, where the two subunits were encoded by a bicistronic construct[7, 10] co-expressed in E. coli with a shortened Taspase1 loop (ESI Fig. S2). Moreover, we made use of an inactive version of Taspase1 where mutations in the active site (D233A and T234A) prevent autocatalytic activation. To ensure full functionality of all proteins used in the study, NiNTA affinity purification and subsequent preparative and analytical gel filtration were followed by SDS-PAGE (ESI Fig. S2), far-UV CD spectroscopy, tryptophan fluorescence melting curves (ESI Fig. S3), MALDI-TOF mass spectrometry (ESI Fig. S4) and validation of proteolytic activity (ESI Fig. S5).

Binding of Taspase1 to silica nanoparticles was observed in a microscale thermophoresis (MST) experiment (Fig. 1a). Here,

View Article Online
DOI: 10.1039/D0NR01637D

Taspase1 was added to silica nanoparticles with 8 (Amsil 8) or 125 nm (Amsil 125) diameter, and high affinity binding was observed in solution. The obtained EC50 concentrations were in the nanomolar range for Amsil8 (35 nM ± 0.5 nM) and in the picomolar range for Amsil125 (10 pM ± 0.4 pM).

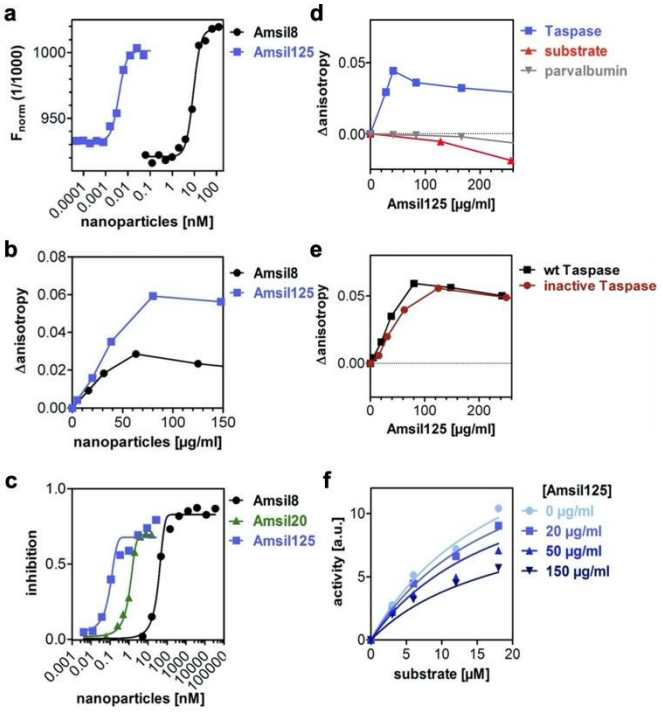

Figure 1. Nanoparticles bind and inhibit Taspase1 noncompetitively. a) Binding of Taspase1 to nanoparticles is deduced from Microscale thermophoresis (MST) dose-response curves. For 8 nm (Amsil8) and 125 nm (Amsil125) silica nanoparticles EC50 values of 35 nM ± 0.5 nM and 10 pM ± 0.4 pM were obtained. b) Fluorescence anisotropy binding isotherms using 1 µM Atto488-labeled Taspase1 reveal a stoichiometry of roughly 10 µmol/mg nanoparticles, which corresponds to about 6 Taspase1 molecules per Amsil8 nanoparticle and approximately 5000 Taspase1 molecules per Amsil125 nanoparticle. c) Taspase1 activity is inhibited by silica nanoparticles. For particles with a diameter of 8 nm (Amsil8), 20 nm (Amsil20) and 125 nm (Amsil125) nm IC50 values of 41 ± 9 nM, 1.4 ± 0.3 nM and 119 ± 21 pM were calculated, respectively. d) Influence of Amsil125 on fluorescence anisotropy signals of various proteins. While the signal for Atto488-labeled Taspase1 undergoes a significant increase on addition of nanoparticles, the anisotropies of the fluorogenic substrate and the Atto488-labeled control protein (parvalbumin) alter only marginally. e) The striking resemblance in anisotropy changes of Atto488-labeled wild-type Taspase1 (wt; data taken from b) to the inactive Taspase1 mutant (red) upon addition of Amsil125 nanoparticles indicate similar binding modes. f) Decline of Taspase1 activity upon addition of rising amounts of Amsil125 at different substrate concentrations pinpoints towards a noncompetitive inhibition mechanism (R2 = 0.98). A Ki value of 380 ± 55 pM could be calculated.

Active site fluorescence anisotropy titrations with Atto488-labeled Taspase1 confirmed the ranges of binding affinities detected by MST and displayed a higher change in anisotropy upon binding for Amsil125 than for Amsil8 due to the higher molecular weight (Fig. 1b). Based on these data, a stoichiometry of roughly 10 nmol per mg nanoparticles was calculated for both, Amsil8 and Amsil125. This corresponds to approximately 6 Taspase1 molecules bound per Amsil8 and 5000 Taspase1 molecules per Amsil125 particle. Next, we explored possible consequences of nanoparticle adhesion on Taspase1 activity by an in vitro assay (Fig. 1c; ESI Fig. S5a,b) using a substrate based on Taspase1's preferred MLL cleavage sequence CS2 (ESI Fig. S5e, ESI Table S6). All silica nanoparticles tested (8, 20 and 125 nm in diameter) inhibited Taspase1 activity already at low concentrations. As observed for binding to nanoparticles, the EC50 concentrations negatively correlate with the particle diameter. Hence, Amsil125 displays the lowest IC50 value with 119 ± 21 pM, while Amsil20 and Amsil8 inhibit Taspase1 at nanomolar concentrations (IC50 = 1.4 ± 0.3 nM and 41 ± 9 nM, respectively). However, nanoparticles would artificially lower Taspase1 activity if they bind the fluorescent substrate and render it unavailable for Taspase1 cleavage. Therefore, we compared substrate peptide and Taspase1 binding to Amsil125 using fluorescence anisotropy (Fig. 1d). While the anisotropy of Taspase1 changed upon binding to nanoparticles, the virtually constant anisotropy of the substrate excluded binding of the substrate to nanoparticles. Furthermore, the constant anisotropy of the Atto488-labeled control protein parvalbumin excludes that the Atto488 dye mediates binding to nanoparticles. Binding of parvalbumin to nanoparticles could be observed only at higher concentrations. However, the EC50 value of 3 ± 0.8 µM determined for this interaction is 300 000-fold higher compared to Taspase1. Interestingly, the proenzyme binds to Amsil125 comparable to the wild-type enzyme as revealed by titration experiments with an Atto488-labeled inactive Taspase1 mutant (Fig. 1e). To gain first mechanistic insights, the inhibition type was determined for Amsil125 by a variation of both substrate and NP concentrations (Fig. 1f). Nonlinear fitting reveals a reversible noncompetitive inhibition with a Ki value of 380 ± 55 pM which might be indicative for a destabilization and thus unfolding of Taspase1 by nanoparticles. Hence, the impact of nanoparticles on the secondary structure of Taspase1 was analyzed via CD spectroscopy (Fig. 2). Melting curve analysis reveals a melting temperature (T_m) of 59 °C for wild-type Taspase1, which consists of α- and β-subunit, and a T_m of 60 °C for the active Taspase1 variant (ESI Fig. S3c). The somewhat higher T_m of the inactive mutant might be due to its continuous polypeptide chain. The far-UV CD spectra obtained in the presence and absence of nanoparticles are indistinguishable, indicating that neither nanoparticle type caused a change in secondary structure composition at inhibitory concentrations of 40 µg/ml (Fig. 2a). Of note, no structural changes could be observed up to a concentration of 150 µg/ml for Amsil20 (ESI Fig. S3e). First concentration-dependent effects are however detectable at extremely high Amsil20 concentrations (300 and 600 µg/ml) that have not been used in any other experimental setup of this study (data not shown).

However, these data cannot exclude a change in tertiary structure, such as a movement or torsion of a whole subunit. Consequently, fluorescence tryptophan melting curves were recorded to get insight into the tertiary structure, as well as the overall folding state and stability of Taspase1 (Fig. 2b).

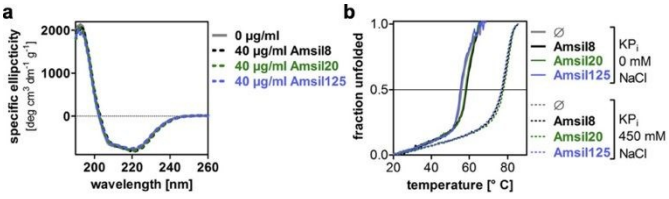

View Article Online
DOI: 10.1039/D0NR01631D

Figure 2. Nanoparticles do not alter secondary structure or stability. a) CD spectra in the presence of nanoparticles. Addition of Amisil8, Amisil20 or Amisil125 do not change the secondary structure of Taspase1. b) Melting curves upon addition of nanoparticles followed by tryptophan fluorescence. No significant change within the stability of Taspase 1 is observed, as the corresponding melting points, both in the presence and absence of 100 µg/ml nanoparticles with 8 nm (Amsil8), 20 nm (Amsil20) and 125 nm (Amsil125) diameter, remain close to 56 °C (phosphate buffer without NaCl (solid lines)) or close to 77 °C (phosphate buffer with 450 mM NaCl (dashed lines)), respectively.

Fluorescence spectroscopy yielded a melting temperature of 56 °C for wild-type Taspase1 (ESI Fig. S3d). As expected, the known stabilizing effect of sucrose and chloride on Taspase1[7, 10] was also mirrored by an increase of the T_m by 17 °C and 21 °C upon addition of sucrose or NaCl, respectively. Irrespective of the salt concentration, melting temperatures do not change in the presence of 100 µg/ml nanoparticles, corresponding to 266 nM for Amsil8, 16 nM for Amsil20, and 204 pM for Amsil125, respectively (Fig. 2b). Taken together, these data argue against changes in secondary or tertiary structure and indicate that the inhibitory effect of the silica nanoparticles on Taspase1 is not caused by destabilization.

Enzyme inhibition is no general feature of nanoparticles.

Theoretically, inhibition of enzyme activity might be not only restricted to Taspase1, but might instead be a general feature of nanoparticles. To test the hypothesis, three control enzymes were studied in activity assays (Fig. 3).

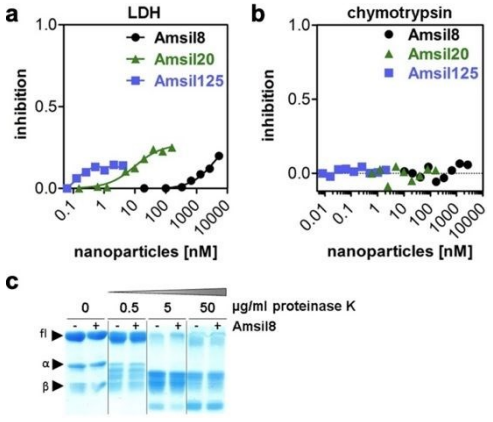

Figure 3. LDH, chymotrypsin and proteinase K are weakly inhibited by nanoparticles. a) Lactate dehydrogenase (LDH) activity in the presence of silica nanoparticles Amsil8 displays only negligible inhibition at high concentrations (3 mg/ml), whereas Amsil20 and Amsil125 inhibit activity with a nanomolar EC50 by up to 25 % and 15 %, respectively. b) Chymotrypsin activity remains unaffected upon addition of nanoparticles with 8 nm, (Amsil8), 20 nm (Amsil20) and 125 nm (Amsil125) diameter. c) Proteinase K activity is not influenced by nanoparticles. For proteinase K concentrations between 0.05 and 50 µg/ml, the digestion pattern does not change in the presence of 100 µg/ml Amsil8. Arrows indicate the size of full-length Taspase1 (fl), as well as those of the α- and β-subunits. Lines separate lanes from different gel runs.

First, lactate formation by lactate dehydrogenase (LDH) was assayed; second, the serine endopeptidase chymotrypsin was assayed for proteolytic activity; and third, the serine endo- and exopeptidase proteinase K was tested for proteolysis in the presence of nanoparticles. Amsil125 inhibits LDH activity by up to 15 % at low nanomolar concentrations (Fig. 3a). Of note, higher concentrations cause no further reduction of LDH activity. For Amsil20, inhibition is not seen in the picomolar range, where Taspase1 is already significantly inhibited. However, higher concentrations can reduce LDH activity by up to 25 %. Similarly, micromolar concentrations of Amsil8 are required to inhibit LDH activity by 10 %, which is two orders of magnitude more than for Taspase1 inhibition with an EC50 value of 41 nM. Thus, the nanoparticle concentrations required for LDH inhibition are 1-2 orders of magnitude higher than for Taspase1. Moreover, nanoparticles cannot reduce LDH activity by more than 25 %, in contrast to the 90 % inhibition observed for Taspase1. Regarding chymotrypsin, enzymatic activity is not affected by nanoparticles, regardless of size and concentration even if exceeding the EC50 of Taspase1 by two orders of magnitude (Fig. 3b). To assay the activity of proteinase K, the Taspase1 digestion pattern was analysed by SDS-PAGE after limited proteolysis by proteinase K (Fig. 3c). The digestion bands visible below both the full-length enzyme and the two subunits indicate that high concentrations of proteinase K are indeed able to degrade all three Taspase1 species. A comparison of the degradation pattern in the presence and absence of 100 µg/ml Amsi8 reveals no inhibition for all proteinase K concentrations tested.

Nanoparticles inhibit Taspase1 in cell lysates and in cells.

Next, we set out to elucidate possible effects of nanoparticles on Taspase1 activity in the more physiological environment of a whole cell lysate, where the complete cellular proteome is present. Here, we used Hela cell lysates with overexpressed GFP-Taspase1 (Fig. 4a). Of note, as explicated above, although sodium chloride stabilizes Taspase1 and prevents precipitation (ESI Fig. S3d, Supplementary Information), chloride inhibits Taspase1 activity with an IC_{50} value of 68 ± 7 mM (data not shown). Hence, chloride was replaced by sucrose as stabilizing agent. Strikingly, nanoparticles reduce the activity of overexpressed Taspase1 only by up to 50 % in lysates. Moreover, the EC_{50} values (40-250 µg/ml) are somewhat higher than for pure, recombinant Taspase1 (8-60 µg/ml). Indeed, various parameters might contribute to a lower inhibitory effect, most likely nanoparticle binding to other proteins or macromolecules present in the lysate. Partially, this could be counteracted by the overexpression setting that elevates the amount of Taspase1 presumably by some orders of magnitude.[31] Thus, the inhibitory concentrations measured in cell lysates were still in the nanomolar and sub-nanomolar range. As cellular uptake of nanoparticles is regarded a critical step when it comes to their biomedical use, we consequently tested the effect of nanoparticles on Taspase1 activity inside living cells. As there are almost 30 different physiological substrates including many transcription factors, it would be extremely challenging or even impossible to reliably quantify cleavage of specific endogenous target proteins. In line with previous studies focusing on the identification of Taspase1 inhibitors,[14, 32] we thus made use of a suited cleavage reporter for cell transfection. Our cell-based activity assay employs a eukaryotic fluorescent reporter substrate, called BioTasp,[12, 14] equipped with nuclear import (NLS)- and export (NES) sequences (Fig. 4b). Following cellular overexpression, BioTasp shuttles between nucleus and cytoplasm, but localizes

predominantly to the cytoplasm, since the NES activity is dominant over the NLS. As expected, co-expression of proteolytically active Taspase1 triggers nuclear accumulation of the biosensor by removing the NES sequence, while co-expression of inactive Taspase1 has no effect (Fig. 4c). Statistical evaluation confirmed a significantly increased nuclear localization in cells with active Taspase1 compared to cells overexpressing the inactive or no protease (Fig. 4d).

Figure 4. Nanoparticles inhibit Taspase1 activity in cell lysates and in live cells. a) Taspase1 activity was assayed in HeLa cell lysates in the presence of Amsil8, Amsil20 and Amsil125. EC50 values of 80 ± 34 µg/ml (= 213 ± 90 nM) for Amsil8, 251 ± 24 µg/ml (= 40 ± 4 nM) for Amsil20 and 42 ± 15 µg/ml (= 86 ± 31 pM) for Amsil125 were calculated by nonlinear fitting. b) Scheme representing the domain/site arrangement within the BioTasp reporter substrate depicting the positions of the N-terminal nuclear localization signal (NLS, grey), the enhanced green fluorescent protein (eGFP, green), the glutathione S-transferase (GST, grey) and the Taspase1 cleavage site (red; scissors) as well as the reverse nuclear export signal (NES, grey). c) Fluorescence microscopy images of HeLa cells. BioTasp (green) localizes predominantly to the cytoplasm, since the NES activity is

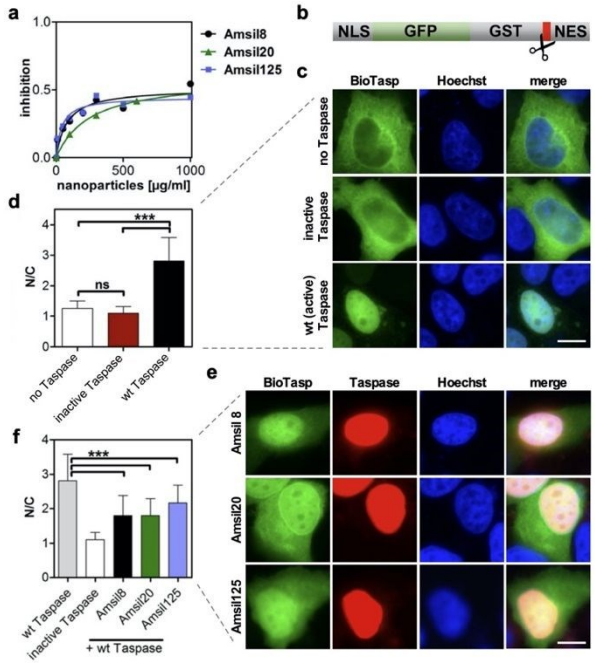

dominant over the NLS (top line). In presence of active wild-type Taspase1 (wt Taspase1; middle line), but not proteolytically inactive Taspase1 (bottom line), the NES is cleaved off and the NLS drives nuclear accumulation of the biosensor. Nuclei were stained with Hoechst (blue). d) Statistical analysis reveals no significant (ns) difference in the nucleus to cytoplasm ratio (N/C) of BioTasp between untransfected cells and cells with inactive Taspase1. In contrast, the N/C ratio is significantly higher in cells overexpressing active wild-type Taspase1. e) Hela cells transfected with Taspase1 C-terminally fused to mCherry (red) and the BioTasp reporter (green) were incubated with 200 µg/ml Amsil8, Amsil20 or Amsil125 for 18 h before Hoechst nuclear staining (blue). Nanoparticle treatment efficiently counteracted the nuclear accumulation of the biosensor by inhibiting Taspase1 proteolytic activity. f) Statistical analysis of the nucleus to cytoplasm ratio (N/C) reveals a significantly reduced N/C ratio in the presence of nanoparticles compared to untreated controls. For d) and f) 50 cells from 3 independent experiments were analysed. *** indicate p values < 0.001. Scale Bars, 20 µm.

We now applied this assay to test the inhibitory potential of the silica nanoparticles (8, 20 and 125 nm diameter) in a cellular environment (Fig. 4e). For this, HeLa cells were incubated with 200 µg/ml nanoparticles 3 h after transfection with Taspase1. Successful overexpression of active Taspase1 and correct nuclear localization were controlled by fluorescence microscopy (Fig. 4e). After 18 h of incubation, the localization of the BioTasp sensor was analyzed. Of note, presence of nanoparticles had no visible effect on cell viability or morphology. Indeed, nanoparticle treatment efficiently counteracted the nuclear accumulation of the biosensor, as also evident from the statistical evaluation (Fig. 4f). At a concentration of 200 µg/ml, nanoparticles significantly reduced Taspase1 activity in Hela cells by roughly 50 %, with the inhibitory effect of Amsil8 and Amsil20 somewhat less pronounced compared to Amsil8 and Amsil20.

Discussion

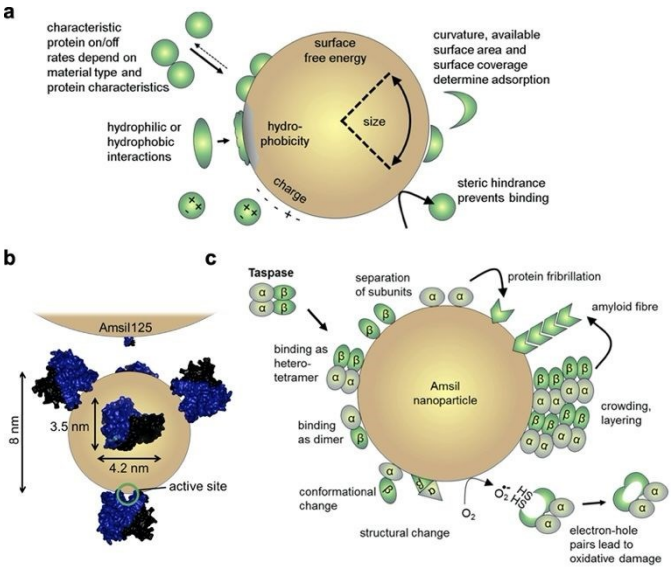

In physiological environments, proteins and other biomolecules rapidly bind to nanomaterials, forming a biomolecule corona that critically affects the physico-chemical properties and thus the (patho)biological behaviour of the adsorbed molecules. On the other hand, adsorption might also influence the biological properties and cellular function of the adsorbed biomolecules.[1] However, most of the recent experimental approaches focused on the effects and consequences for the nanomaterials instead of the bound proteins. Nevertheless, there is already evidence that binding of certain nanoparticles to a still rather limited number of enzymes indeed affects their enzymatic activity.[22-29] Interestingly, it is possible to functionally modulate the proteasome, a very important molecular machine, by nanomaterials.[26] Regarding the similarities of the proteolytic mechanisms between the 20S proteasome and the oncologically relevant Threonine protease Taspase1,[7] it was tempting to speculate that Taspase1 might be also affected by nanoparticle binding. Admittedly, Taspase1's catalytic activity is not affected by common protease inhibitors.[7] However, as neither genetic nor specific and highly effective chemical inhibitors are available for this enzyme, the exploitation of novel interference strategies for Taspase1 is of utmost importance.[18, 19] In this study, we primarily focused on the direct effects of adsorption onto the protein surface, and thus decided to make use of only a small set of amorphous silica-based nanoparticles. These particles are already very well characterized in different comprehensive studies[33, 34] and do not exhibit an intrinsically high cellular toxicity. Indeed, microscale thermophoresis and fluorescence anisotropy experiments revealed binding of Taspase1 to silica nanoparticles at low nanomolar concentrations. Importantly, the control protein parvalbumin showed a 300 000-fold weaker affinity. To understand why some proteins bind to nanoparticles with particularly high affinity, the protein-nanoparticle interface needs to be examined in more detail. Despite extensive research in recent years, the interactions of nanoparticles with biomolecules are still not fully elucidated. However, some concepts emerged from these efforts,[35] which help understand the influence of nanoparticles on proteins (Fig. 5a).

Figure 5. a) Interactions of proteins with nanoparticles. Binding to nanoparticles (brown) is dependent on protein-specific on/off rates, as well as hydrophobicity, size and charge of the particles. Green circles represent various proteins. Modified according to Nel et al., 2009.[35] b) True-to-scale model of Taspase1 bound to nanoparticles. Size comparison of Taspase1 and Amsil125 and scaled model of Taspase1 bound to Amsil8 nanoparticles as ??-heterodimer (black and blue, respectively). The active site (green circle) is occluded in the bound state. The calculated stoichiometry of 6:1 is displayed. c) Structural changes of proteins bound on nanoparticles as exemplified for Taspase1 subunits (green circles). Models for Taspase1 inhibition by nanoparticles include steric occlusion of the active site after binding as hetero-tetramer or dimer, separation of the subunits, as well as structural or conformational changes, crowding effects, fibrillation and oxidation. Modified according to Nel et al., 2009.[35]

Obvious factors that govern the interactions are charge distribution and hydrophobicity of the particle and the protein. Surprisingly, negatively charged proteins show increased binding to nanoparticles, irrespective of their net charge.[33] Other important determinants are the size and curvature of the nanoparticles and steric factors, rendering the protein corona

on the particle surface specific for each type of nanomaterial. Hence, nanoparticles indeed interact selectively with distinct subsets of proteins and do not bind every biomolecule.[33, 34] This is in perfect agreement with our current observation that Taspase1 binds to negatively charged amorphous silica nanoparticles while parvalbumin is rejected. Even more, our experiments revealed that surface area and curvature of the particles significantly impact Taspase1 binding affinity and capacity. The EC50 of nanoparticles with a diameter of 125 nm (Amsil125) is 3500-fold lower compared to nanoparticles of 8 nm diameter (Amsil8), reflected in a calculated stoichiometry of roughly 5000 and 6 Taspase1 molecules per Amsil125 and Amsil8 nanoparticle, respectively (Fig. 5b). This agrees with the stoichiometry of 620:1 reported for HSA with 70 nm NIPAM/BAM-nanoparticles.[36] Notably, an Amsil8 particle binds roughly 800 times less Taspase1 molecules than an Amsil125 particle, although the surface area is only around 250 times smaller. This might probably be attributed to Taspase1's ability to bind with higher density to a surface with low curvature (Amsil125) than to highly curved surfaces (Amsil8).

Here, we could demonstrate for the first time that amorphous silica nanoparticles not only bind, but also inhibit Taspase1's proteolytic activity. Notably, binding and inhibition occur at similar nanoparticle concentrations, indicating that every Taspase1 molecule bound to a nanoparticle is more or less severely compromised in its biological activity. However, the phenomenon of enzyme inhibition by nanoparticles is still poorly investigated and scarcely described in literature. Examples are the inhibition of chymotrypsin and trypsin by multi-walled carbon nanotubes, which were specifically imprinted to enable enzyme binding,[22,23] Another study investigating the influence of single-walled carbon nanotubes revealed an irreversible inhibition of chymotrypsin activity and more than 90 % inhibition of soybean peroxidase activity.[37] Regarding the underlying mechanism, the authors suggested a denaturation of chymotrypsin, while the mechanism for soybean peroxidase inhibition remained unresolved. Emanating from these hypotheses and the concepts developed by Nel et al.[35], we considered different mechanistic scenarios that might account for enzymatic inhibition of Taspase1 by nanoparticles (Fig. 5c). These included structural or conformational changes, oxidative processes, crowding and layering, protein fibrillation and different binding modes of the Taspase1's dimer, hetero-tetramer or separated protease subunits. Structural changes have been described for the human β2-microglobulin upon binding to copolymer particles, cerium oxide particles, quantum dots and nanotubes, and were based on nucleation of protein fibrils and thereby induce amyloid formation.[38] However, the secondary structure of Taspase1 is not altered upon binding to nanoparticles, and also the reversibility of the inhibition does not agree with an irreversible fibrillation and aggregation process. Moreover, the stability of enzymes bound to nanoparticles can differ from the enzyme in solution.[37, 39] Interestingly, this effect can either be stabilizing or destabilizing, depending on both the nature of the particle (e.g., spherical or tube-like shape) and the adsorbed protein. Additionally, the storage stability of glucose oxidase was significantly increased after binding to silica-encapsulated magnetic nanoparticles.[40] Nevertheless, both stabilization and destabilization can be excluded as the cause for Taspase1 inhibition, since its stability is clearly not altered by nanoparticle addition. Oxidation of Taspase1 catalysed by nanoparticles, as already described for other biomolecules,[41-43] is also unlikely due to the highly reducing milieu in the buffer containing 10 mM DTT. Moreover, binding of proteins to nanoparticles can greatly increase the local protein concentration in the corona and cause layering or crowding effects, which are known to promote aggregation.[44, 45] Indeed, the stoichiometry of 6 and 5000 Taspase1 molecules per Amsil8 and Amsil125 nanoparticle, respectively, indicates high local Taspase1 concentrations. However, the CD spectra in the presence of nanoparticles argue against the aggregation of Taspase1. Moreover, assuming an interface size of 35 x 42 Å per Taspase1 monomer and perfect steric packing, the surface coverage of Amsil8 is below 50 % and roughly 150 % for Amsil125. This suggests that a heavily curved surface can bind less Taspase1 molecules compared to flatter surfaces (Fig. 5b). However, a burying of Taspase1 by multiple layers in the nanoparticle corona is probably not the cause for the reduced activity. Based on our current data, the most plausible explanation for Taspase1 inhibition by nanoparticles is binding as an αβ-dimer in a single layer without conformational change (Fig. 5c). This might result in noncompetitive inhibition that is either allostery-like or occludes the active site. However, the latter mechanism is more likely, since Taspase1's positively charged active site is probably part of the binding interface for the strongly negatively charged nanoparticles. As a result, the active site is reversibly occluded and inaccessible for the substrate. Given the fact that the inactive mutant can still interact with nanoparticles, the positively charged Taspase1 loop (pI = 9.8) most likely supports binding independently of its location. Finally, separation of the αβ-dimer and binding of only one of the two conversely charged subunits can be ruled out, as this would result in free α- or β-subunits (25 and 20 kDa, respectively), which again can be excluded since neither subunit is found after filtration through a 30 kDa membrane (data not shown).

Importantly, control experiments with lactate dehydrogenase, chymotrypsin and proteinase K showed no or little inhibition of the respective enzyme activity at nanoparticle concentrations needed for Taspase1 inhibition. Nanoparticle concentrations required for LDH inhibition are 1-2 orders of magnitude higher than for Taspase1, and no inhibitory effect was found for chymotrypsin and proteinase K. Moreover, nanoparticles cannot reduce LDH activity by more than 25 %, in contrast to 90 % inhibition seen with Taspase1. This pinpoints that silica nanoparticles do not inhibit enzymes in general and might even suggest a preference for a certain catalytic type of proteases. While the silica nanoparticles displayed an inhibitory effect on the threonine protease Taspase1, they failed to inhibit the serine proteases chymotrypsin and proteinase K. This agrees with the finding that nanoparticles indeed bind selective sets of proteins.[33] However, to rationally predict whether an enzyme is inhibited by a certain type of nanoparticle, further studies are urgently required to gain a deeper understanding of the

underlying interaction mechanisms. In contrast to the in vitro situation where the recombinant protein is predominant, in physiological environments a large variety of different proteins compete for binding to the nanoparticle protein corona. To mimic such conditions, HeLa cell lysates with overexpressed GFP-Taspase1 were tested in the presence of silica nanoparticles. While nanoparticles were able to inhibit Taspase1 by up to 90 % in vitro, the maximum inhibitory effect is limited to 50 % in cell lysates. Consequently, the nanoparticle surface might be partly occupied by other cellular proteins, which reduce the inhibitory potential with respect to Taspase1. Nevertheless, our results revealed a nanomolar affinity also in cell lysates, which prompted us to further investigate Taspase1 inhibition in living cells. Owing to their large size, nanoparticles cannot enter the cell passively, but must be taken up actively. However, uptake efficiency crucially depends on size and shape of the nanoparticle.[46] The current mechanistic model involves energy-dependent wrapping of the nanoparticle with the help of clathrin and the cytoskeleton.[35] Tissue-specific targeting of compounds could e.g. be achieved by coating nanoparticles with lung-targeting peptides, which resulted in an enrichment of these nanoparticles in the lung after venous injection in mice.[47] Even targeting of cellular compartments was successfully conducted in living cells with nanoparticles conjugated to a small signal peptide. With this approach, fluorescent nanocrystal quantum dots accumulated selectively in the mitochondria or the nucleus within 15 minutes.[48] Some nanoparticles pose a risk to cells due to their toxic potential. Especially crystalline silica is known to induce chronic inflammation, fibrosis and lung cancer upon inhalation.[49, 50] In sharp contrast to the high toxicity of crystalline silica, amorphous silica nanoparticles are regarded to be safe without displaying chronic effects, as studied in rats.[51] This agrees with the good viability of the cells after Amsil nanoparticle challenge - including normal proliferation, cell size and morphology. In a previous study, we already demonstrated that fluorescently labelled silica nanoparticles were readily taken up within roughly one hour, and uptake efficiency was increased in the presence of serum.[33] However, in contrast to the biochemical data clearly showing that binding and inhibitory potential correlate with the particle diameter, this effect is not obvious in the cell-based assay. In addition to the parameters regarding differences in particle uptake and thus biocompatibility, such assays are *per se* not able to provide the sensitivity of a biochemical test. Particularly, protein concentrations may vary in different cells, depending on the level of overexpression and maybe also on cell-cycle-dependent post-translational protein modifications (PTMs), which cannot be determined as precisely as the amount of (active) enzyme in a recombinant setting. In addition, larger particles might be disadvantaged regarding cellular uptake, thereby lessening their inhibitory potential as observed in the biochemical assays. Of note, Taspase1's nuclear localization, established by a dynamic interplay between the import receptor importin-α and nucleophosmin,[11] is also retained in the presence of nanoparticles. Finally, the sum of effects described above may counteract the contribution of size-dependency on inhibition.

An undoubtedly exciting line of current biomedical research is the inhibition of enzymes by blood-circulating nanoparticles for tumor therapy.[52-54] Although our recent data suggest a direct interaction of Taspase1 with the surface of silica nanoparticles, it would as well be of interest to assess preceding association with other proteins. Further work could e.g. investigate pre-incubation of particles with proteins of the blood serum and subsequent incubation with Taspase1 and other oncologically relevant enzymes. Thus, we hope to stimulate similar studies involving also other types of nanomaterials and biomolecules to get closer to the "big picture" of nanoparticle-induced cellular processes. Albeit we are well aware that further experimental proof is required, it is tempting to speculate that the principle identified here is of general biological relevance for different research disciplines.

Experimental

Nanoparticles

Aqueous dispersions of amorphous silica (silicon dioxide, SiO_2) nanoparticles (Amsil-NP) of different diameter (Amsil8, ∅8 nm; Amsil20, ∅20 nm; Amsil125, ∅125 nm) were purchased from Nyacol Nano Technologies (Ashland). The Amsil-NP were diluted with water and characterized with respect to shape, size, and size distribution in the dry state as well as in solution at 25 °C at a concentration of 0.6 mg/ml by transmission electron microscopy (TEM) imaging and dynamic light scattering (DLS) analysis as described (ESI Table S1).[33]

Microscale thermophoresis (MST) measurements

Taspase1 was labeled with cysteine-reactive Atto488 dye (Atto-Tec) in 50 mM NaH_2PO_4 pH 8, 450 mM NaCl. 50 nM labeled Taspase1 was briefly incubated with indicated nanoparticles in a buffer containing 50 mM NaH_2PO_4 pH 8.0, 450 mM NaCl, 1 mM DTT, 0.1 % Tween and loaded into glass capillaries. Measurements were taken in a Monolith NT.115 (NanoTemper) with a temperature gradient of 4 °C. Nonlinear curve fitting was performed in GraphPad Prism 5.1 (GraphPad Software) using the built-in equations.

Fluorescence anisotropy measurements

Taspase1 variants and the control protein parvalbumin were N-terminally labeled with Atto488-maleimide (Atto-Tec) in 50 mM NaH_2PO_4, 450 mM NaCl, pH 7.4 (refer to Supporting Information for details). Fluorescence anisotropy was measured with a Varian Cary Eclipse spectrofluorometer (Agilent Technologies) equipped with polarizer wheels. Readings were taken at 20 °C with 1 µM labeled protein in 60 µl of 50 mM NaH_2PO_4, 450 mM NaCl, 1 mM DTT, pH 8, using 3 mm cuvettes (Hellma) and averaged over 5 min, with all parameters kept constant (ESI Table S2). Nonlinear curve fitting of absolute anisotropy changes was performed in GraphPad Prism 5.1.

Fluorogenic in vitro activity assay

The CS2 cleavage site from MLL was synthesized with an N-terminal anthranilic acid (Abz) and a C-terminal dinitrophenol (DNP) quencher, yielding [Abz]-KISQLDGVDDK-[DNP] (CASLO ApS) as fluorescent substrate. 300 nM purified Taspase1 were added to 8 µM substrate in 60 µl 100 mM HEPES pH 7.9, 10 % sucrose, 10 mM DTT. The increase in fluorescence emission at 420 nm due to separation of dye and quencher was followed at 37 °C in a Varian Cary Eclipse spectrofluorometer (Agilent Technologies) after excitation at 320 nm with the settings provided (ESI Table S3). For lysate activity assays, HeLa Kyoto cells were lysed one day after transfection of pTaspase-GFP in 25 mM Tris pH 7.4, 150 mM KCl, 5 mM MgCl2, 5 % glycerol, 1 % triton X-100, 2 mM 2-mercaptoethanol, 1 mM PMSF and 1 cOmplete protease inhibitor cocktail tablet. 8 µM substrate was added to 60 µl of total cell lysate, and substrate cleavage was measured by monitoring the fluorescence recovery of the quenched dye at 30 °C and compared to untransfected lysate.

CD spectrometry. Far-UV spectra were recorded on a Jasco J-710 spectropolarimeter (Jasco Analytical Instruments). CD intensities are presented as molar ellipticity ($cm^3\ dm^{-1}\ g^{-1}$). Measurements were taken with 0.2 mg/ml Taspase1 in 50 mM NaH_2PO_4 pH 6.5, with all parameters kept constant (ESI Table S4). Spectra were baseline-corrected by subtraction of a buffer spectrum using cuvettes with 1 mm path length (Hellma).

Fluorescence melting curves

For fluorescence melting curves, the red-shift of tryptophan emission upon unfolding was exploited for 10 µM Taspase1 in a total volume of 200 µl as described [55], with all parameters kept constant (ESI Table S5). The difference in intensities was normalized according to the equation $D = I{\downarrow}334 - I{\downarrow}376/I{\downarrow}334 + I{\downarrow}376$, where I represents the fluorescence intensities at 334 nm and 376 nm, respectively.

Enzymatic assays

All enzymatic assays were measured in a Varian Cary 100 spectrophotometer (Varian) at indicated wavelength. To assay lactate dehydrogenase (LDH; Sigma-Aldrich) activity, the conversion of NADH to NAD^+ during the reduction of pyruvate to lactate was followed at 340 nm. LDH was added in a final concentration of 100 ng/µl to start the reaction. Substrates were present in saturating concentrations of 250 µM NADH and 1 mM pyruvate in 100 mM NaH_2PO_4 pH 7.4. Measurements were performed with a spectral band width of 1 nm and 5 sec average time at 20 °C. Prior to each measurement, the blank rate of 250 µM NADH and 1 mM pyruvate in 100 mM sodium phosphate buffer pH 7.4 was measured for 2 min. With a molar extinction coefficient of 6220 $M^{-1}\ cm^{-1}$ for NADH, the NADH consumption per minute was calculated and the blank rate was subtracted. To test for inhibition, Amsil8 and Amsil125 nanoparticles were added to the final reaction volume of 300 µl and incubated briefly, before the activity was assayed. Cleavage of 150 µM substrate peptide ([succinyl]-A-S-P-F-[4-nitroaniline]; Bachem) by 350 nM Chymotrypsin (Sigma-Aldrich) at 20 °C in 300 µl of 50 mM NaH_2PO_4 pH 8.0, 10 % sucrose, 450 mM NaCl, 1 m DTT was followed at 390 nm. First, the blank rate of 150 µM substrate peptide in presence or absence of nanoparticles was followed for 2 min, before the reaction was started by addition of 350 nM chymotrypsin. After baseline subtraction, the comparison of the linear increase in absorbance with and without nanoparticles allowed a determination of the inhibitory effect. For stability assays, 6 µg of Taspase1 were digested by Proteinase K (0.05-100 µg/ml; New England Biolabs) in presence or absence of 100 µg/ml of the indicated nanoparticles in 50 mM NaH_2PO_4 pH 8, 450 mM NaCl, 1 mM DTT. After incubation at 20 °C for 10 min, the reaction was stopped by adding of 1 mM PMSF, and protein fragments were separated by SDS-PAGE and stained with Coomassie.

Cell culture, transfection and cellular activity assay

Human cervix epithelial HeLa Kyoto cells (ATCC-No. CCL-2) were maintained as recommended by the American Type Culture Collection (ATCC) in complete Dulbecco`s Modified Eagle Medium (DMEM) supplemented with 10 % fetal bovine serum, 1 % Glutamine and 1 % Antibiotic-Antimycotic (Invitrogen) at 37° C in a humidified atmosphere of 5 % CO_2. $2x10^5$ cells were seeded on cover slips and transfected 24 h after seeding with 1 µg plasmid DNA encoding Taspase1-mCherry and BioTasp using XtremeGene (Roche) following the manufacturer's instructions. Cells were challenged with 200 µg/ml nanoparticles 3 h after transfection, incubated for 18 h, fixed, and nuclei were stained with 1 µg/ml Hoechst. Fluorescence microscopy images were taken on an Olympus BX61 microscope (Olympus) with constant channel settings (ESI Table S7) and analyzed with the open source software ImageJ. Cell borders were identified via the respective brightfield images and autofluorescence, while nuclei were defined using the DAPI channel. Intensity ratios of nucleus to cytoplasm were calculated, statistically evaluated with GraphPad Prism 5.03 (GraphPad Software, 2009), and an unpaired student's t-test was applied.

Conclusions

Altogether, the inhibition of Taspase1 by silica nanoparticles at nanomolar concentrations highlights for the first time that nanoparticles are able to qualitatively inhibit enzymes in vivo. Thus, our study contributes to the comprehension of nanoparticle interactions in living cells. Although the nature of silica nanoparticles does not suggest a selective inhibition, this effect does not apply to proteases in general. However, possible inhibitory effects of nanoparticles on enzymes need to be considered in future studies with regards to possible medical applications. On the other hand, in analogy to the well-established concept of 'biologicals' or 'biologics'[56] it is tempting to speculate that engineered particles will ultimately allow one to rationally manipulate relevant biomolecules. Current nanomedical applications are mostly restricted to imaging, implant functionalization or drug delivery, often relying on additional laborious (bio)molecular functionalization of the nanomaterial (of chemical and/or biological origin) to obtain specificity and the desired activity.[1] In contrast, as part of this

novel concept of 'nanologicals', target specificity and activity are exclusively conferred by the physico-chemical characteristics of the respective nanomaterial, such as size, geometry, charge, roughness and/or surface energy. Such nanomaterial-specific targeting of molecular machines may indeed be of high translational relevance for biotechnology and nanomedicine applications.

Conflicts of interest

There are no conflicts to declare.

Acknowledgements

This work was supported by the Chemical Industry Fund of the VCI (Verband der Chemischen Industrie) to S.K., the German Research Foundation DFG (to D.D./R.S.) and the foreign experts project of Shanxi Provincial '100 Talents Plan' to R.S. Parts of the data were generated during the doctoral dissertation of J.B. entitled "Novel inhibitors of the protease Taspase1".[57]

Author contributions

D.G. and **J.B.** designed and cloned the expression constructs and expressed and purified Taspase1 together with **F.T.**, **A.M.** and **A.Hö**. **J.B.** fluorescently labelled the proteins. **D.D.** and **S.S.** prepared and characterized the nanoparticles. **J.B.** performed microscale thermophoresis, fluorescence anisotropy and mass spectrometry experiments, measured far-UV CD-spectra and fluorescence melting curves together with **F.T.** and **A.M.** and analyzed the data together with **P.B.** and **S.K.K. J.B.** conducted enzymatic and cellular activity assays, analyzed the data and compiled the figures together with **S.K.K. J.B.**, **S.S.** and **A.He.** wrote the manuscript together with **S.K.K**, who designed the study and supervised the experiments together with **P.B.** and **R.H.S**.

References

1. D. Docter, D. Westmeier, M. Markiewicz, S. Stolte, S. K. Knauer and R. H. Stauber, *Chem Soc Rev*, 2015, **44**, 6094-6121.
2. D. Docter, S. Strieth, D. Westmeier, O. Hayden, M. Gao, S. K. Knauer and R. H. Stauber, *Nanomedicine (Lond)*, 2015, **10**, 503-519.
3. R. B. Leveson-Gower, C. Mayer and G. Roelfes, *Nat Rev Chem*, 2019, **3**, 687-705.
4. J. S. Bond, *J Biol Chem*, 2019, **294**, 1643-1651.
5. D. Wunsch, A. Hahlbrock, S. Jung, T. Schirmeister, J. van den Boom, O. Schilling, S. K. Knauer and R. H. Stauber, *Oncogene*, 2016, **35**, 3351-3364.
6. M. Drag and G. S. Salvesen, *Nat Rev Drug Discov*, 2010, **9**, 690-701.
7. J. J. Hsieh, E. H. Cheng and S. J. Korsmeyer, *Cell*, 2003, **115**, 293-303.
8. S. Takeda, D. Y. Chen, T. D. Westergard, J. K. Fisher, J. A. Rubens, S. Sasagawa, J. T. Kan, S. J. Korsmeyer, E. H. Cheng and J. J. Hsieh, *Genes Dev*, 2006, **20**, 2397-2409.
9. M. Bochtler, L. Ditzel, M. Groll, C. Hartmann and R. Huber, *Annu Rev Biophys Biomol Struct*, 1999, **28**, 295-317.
10. J. A. Khan, B. M. Dunn and L. Tong, *Structure*, 2005, **13**, 1443-1452.
11. C. Bier, S. K. Knauer, D. Docter, G. Schneider, O. H. Kramer and R. H. Stauber, *Traffic*, 2011, **12**, 703-714.
12. C. Bier, S. K. Knauer, A. Klapthor, A. Schweitzer, A. Rekik, O. H. Kramer, R. Marschalek and R. H. Stauber, *J Biol Chem*, 2011, **286**, 3007-3017.
13. C. Bier, R. Hecht, L. Kunst, S. Scheiding, D. Wunsch, D. Goesswein, G. Schneider, O. H. Kramer, S. K. Knauer and R. H. Stauber, *PLoS One*, 2012, **7**, e34142.
14. S. K. Knauer, V. Fetz, J. Rabenstein, S. Friedl, B. Hofmann, S. Sabiani, E. Schroder, L. Kunst, E. Proschak, E. Thines, T. Kindler, G. Schneider, R. Marschalek, R. H. Stauber and C. Bier, *PLoS One*, 2011, **6**, e18253.
15. A. Hahlbrock, D. Goesswein, J. Kunzel, D. Wunsch and R. H. Stauber, *Oral Oncol*, 2016, **54**, e10-12.
16. R. H. Stauber, A. Hahlbrock, S. K. Knauer and D. Wunsch, *FASEB J*, 2016, **30**, 1012-1022.
17. C. Schrenk, V. Fetz, C. Vallet, C. Heiselmayer, E. Schroder, A. Hensel, A. Hahlbrock, D. Wunsch, D. Goesswein, C. Bier, N. Habtemichael, G. Schneider, R. H. Stauber and S. K. Knauer, *J Mol Cell Biol*, 2018, **10**, 33-47.
18. C. Bier, S. K. Knauer, D. Wunsch, L. Kunst, S. Scheiding, M. Kaiser, C. Ottmann, O. H. Kramer and R. H. Stauber, *Faseb J*, 2012, **26**, 3421-3429.
19. D. Wunsch, V. Fetz, D. Heider, S. Tenzer, C. Bier, L. Kunst, S. Knauer and R. Stauber, *Blood Cancer J*, 2012, **2**, e77.
20. V. H. Nguyen and B. J. Lee, *Int J Nanomedicine*, 2017, **12**, 3137-3151.
21. P. Satzer, F. Svec, G. Sekot and A. Jungbauer, *Eng Life Sci*, 2016, **16**, 238-246.
22. D. Zheng, S. K. Vashist, M. M. Dykas, S. Saha, K. Al-Rubeaan, E. Lam, J. H. T. Luong and F. S. Sheu, *Materials (Basel)*, 2013, **6**, 1011-1027.
23. A. Guerreiro, A. Poma, K. Karim, E. Moczko, J. Takarada, I. P. de Vargas-Sansalvador, N. Turner, E. Piletska, C. S. de Magalhaes, N. Glazova, A. Serkova, A. Omelianova and S. Piletsky, *Adv Healthc Mater*, 2014, **3**, 1426-1429.
24. S. H. Cha, J. Hong, M. McGuffie, B. Yeom, J. S. VanEpps and N. A. Kotov, *Acs Nano*, 2015, **9**, 9097-9105.
25. A. L. Lira, R. S. Ferreira, R. J. S. Torquato, M. L. V. Oliva, P. Schuck and A. A. Sousa, *Nanoscale Adv*, 2019, **1**, 378-388.
26. C. A. Falaschetti, T. Paunesku, J. Kurepa, D. Nanavati, S. S. Chou, M. De, M. Song, J. T. Jang, A. Wu, V. P. Dravid, J. Cheon, J. Smalle and G. E. Woloschak, *Acs Nano*, 2013, **7**, 7759-7772.
27. H. Bayraktar, P. S. Ghosh, V. M. Rotello and M. J. Knapp, *Chem Commun*, 2006, DOI: 10.1039/b516096k, 1390-1392.
28. H. Derakhshankhah, M. J. Hajipour, E. Barzegari, A. Lotfabadi, M. Ferdousi, A. A. Saboury, E. P. Ng, M. Raoufi, H. Awala, S. Mintova, R. Dinarvand and M. Mahmoudi, *ACS Appl Mater Interfaces*, 2016, **8**, 30768-30779.
29. T. J. Maccormack, R. J. Clark, M. K. M. Dang, G. B. Ma, J. A. Kelly, J. G. C. Veinot and G. G. Goss, *Nanotoxicology*, 2012, **6**, 514-525.
30. Y. Pan, E. K. Sackmann, K. Wypisniak, M. Hornsby, S. S. Datwani and A. E. Herr, *Sci Rep*, 2016, **6**, 39774.
31. H. Moriya, *Mol Biol Cell*, 2015, **26**, 3932-3939.
32. D. Y. Chen, Y. Lee, B. A. Van Tine, A. C. Searleman, T. D. Westergard, H. Liu, H. C. Tu, S. Takeda, Y. Dong, D. R.

View Article Online
DOI: 10.1039/D0NR01631D

Piwnica-Worms, K. J. Oh, S. J. Korsmeyer, A. Hermone, R. Gussio, R. H. Shoemaker, E. H. Cheng and J. J. Hsieh, *Cancer Res*, 2012, **72**, 736-746.
33. S. Tenzer, D. Docter, J. Kuharev, A. Musyanovych, V. Fetz, R. Hecht, F. Schlenk, D. Fischer, K. Kiouptsi, C. Reinhardt, K. Landfester, H. Schild, M. Maskos, S. K. Knauer and R. H. Stauber, *Nat Nanotechnol*, 2013, **8**, 772-781.
34. S. Tenzer, D. Docter, S. Rosfa, A. Wlodarski, J. Kuharev, A. Rekik, S. K. Knauer, C. Bantz, T. Nawroth, C. Bier, J. Sirirattanapan, W. Mann, L. Treuel, R. Zellner, M. Maskos, H. Schild and R. H. Stauber, *Acs Nano*, 2011, **5**, 7155-7167.
35. A. E. Nel, L. Madler, D. Velegol, T. Xia, E. M. Hoek, P. Somasundaran, F. Klaessig, V. Castranova and M. Thompson, *Nat Mater*, 2009, **8**, 543-557.
36. T. Cedervall, I. Lynch, S. Lindman, T. Berggard, E. Thulin, H. Nilsson, K. A. Dawson and S. Linse, *Proc Natl Acad Sci U S A*, 2007, **104**, 2050-2055.
37. S. S. Karajanagi, A. A. Vertegel, R. S. Kane and J. S. Dordick, *Langmuir*, 2004, **20**, 11594-11599.
38. S. Linse, C. Cabaleiro-Lago, W. F. Xue, I. Lynch, S. Lindman, E. Thulin, S. E. Radford and K. A. Dawson, *Proc Natl Acad Sci U S A*, 2007, **104**, 8691-8696.
39. P. Asuri, S. S. Karajanagi, A. A. Vertegel, J. S. Dordick and R. S. Kane, *J Nanosci Nanotechnol*, 2007, **7**, 1675-1678.
40. K. Ashtari, K. Khajeh, J. Fasihi, P. Ashtari, A. Ramazani and H. Vali, *Int J Biol Macromol*, 2012, **50**, 1063-1069.
41. M. Auffan, W. Achouak, J. Rose, M. A. Roncato, C. Chaneac, D. T. Waite, A. Masion, J. C. Woicik, M. R. Wiesner and J. Y. Bottero, *Environ Sci Technol*, 2008, **42**, 6730-6735.
42. A. Nel, T. Xia, L. Madler and N. Li, *Science*, 2006, **311**, 622-627.
43. R. M. Trueb, *Int J Trichology*, 2009, **1**, 6-14.
44. B. van den Berg, R. J. Ellis and C. M. Dobson, *EMBO J*, 1999, **18**, 6927-6933.
45. R. J. Ellis and A. P. Minton, *Biol Chem*, 2006, **387**, 485-497.
46. P. Decuzzi and M. Ferrari, *Biomaterials*, 2007, **28**, 2915-2922.
47. M. E. Akerman, W. C. Chan, P. Laakkonen, S. N. Bhatia and E. Ruoslahti, *Proc Natl Acad Sci U S A*, 2002, **99**, 12617-12621.
48. A. Hoshino, K. Fujioka, T. Oku, S. Nakamura, M. Suga, Y. Yamaguchi, K. Suzuki, M. Yasuhara and K. Yamamoto, *Microbiol Immunol*, 2004, **48**, 985-994.
49. B. T. Mossman and A. Churg, *Am J Respir Crit Care Med*, 1998, **157**, 1666-1680.
50. J. Ovrevik, M. Lag, P. Schwarze and M. Refsnes, *Toxicol Sci*, 2004, **81**, 480-490.
51. D. B. Warheit, T. A. McHugh and M. A. Hartsky, *Scand J Work Environ Health*, 1995, **21 Suppl 2**, 19-21.
52. N. Bertrand, P. Grenier, M. Mahmoudi, E. M. Lima, E. A. Appel, F. Dormont, J. M. Lim, R. Karnik, R. Langer and O. C. Farokhzad, *Nat Commun*, 2017, **8**, 777.
53. T. J. Maccormack, R. J. Clark, M. K. Dang, G. Ma, J. A. Kelly, J. G. Veinot and G. G. Goss, *Nanotoxicology*, 2012, **6**, 514-525.
54. H. Ye, Z. Shen, L. Yu, M. Wei and Y. Li, *Proc Math Phys Eng Sci*, 2018, **474**, 20170845.
55. J. van den Boom, D. Heider, S. R. Martin, A. Pastore and J. W. Mueller, *J Biol Chem*, 2012, **287**, 17645-17655.
56. P. Declerck, R. Danesi, D. Petersel and I. Jacobs, *Drugs*, 2017, **77**, 671-677.
57. J. van den Boom, 2014.

Table of Contents (TOC)

View Article Online
DOI: 10.1039/D0NR01631D

Adsorption of cellular proteins to nanoparticles leads to the rapid formation of a so-called biomolecule corona, affecting not only the identity of the nanomaterial but also the biological function of the bound proteins. Amorphous silica particles specifically inhibit the proteolytic activity of the oncologically relevant protease Taspase1 in a size-dependent, non-competitive manner in vitro and in a cellular environment.

Keyword: Nanoparticle-induced protease inhibition

J. van den Boom*, A. Hensel, F. Trusch, A. Matena, S. Siemer, D. Guel, D. Docter, A. Höing, P. Bayer, R.H. Stauber, S.K. Knauer*

The Other Side of the Corona: Nanoparticles Inhibit the Protease Taspase1 in a Size-Dependent Manner